

# Josephson Effects in MgB<sub>2</sub> Metal Masked Ion Damage Junctions

Dae-Joon Kang, N. H. Peng, C. Jeynes, R. Webb, H. N. Lee, B. Oh, S. H. Moon, G. Burnell, N. A. Stelmashenko, E. J. Tarte, D. F. Moore, and M. G. Blamire

**Abstract**—We have successfully fabricated high quality Josephson junctions in MgB<sub>2</sub> thin films by a combination of 30 kV focused Ga ion beam nanolithography and 50 keV proton ion beam irradiation. The junctions show resistively shunted junction like current—voltage characteristics with additional excess current. Monte Carlo simulation results for the optimized mask structure and experimental results for the dc and ac Josephson effects are presented. This technique is particularly useful for prototyping devices due to its simplicity and flexibility of fabrication and has a great potential for high-density integration.

**Index Terms**—Focused ion beam, ion implantation, Josephson effects, nanotechnology.

## I. INTRODUCTION

THE recent discovery of superconductivity in a known, simple binary compound, MgB<sub>2</sub>, with a high superconducting transition temperature ( $T_C$ ) of 39 K [1] has initiated worldwide efforts to realize reliable and reproducible Josephson junctions in this material in order to exploit its unique advantageous properties compared to other similar type of materials [2]. To date, several groups have reported the fabrication of Josephson junctions in thin film nanobridges, point contacts, focused ion beam damage, and thin film heterostructures geometries [3]–[8]. Unfortunately, fabrication of manufacturable Josephson junctions in thin MgB<sub>2</sub> films has turned out to be rather difficult because of the relatively poor fabrication control and lack of reliable barrier materials for any multilayer junctions, as well as the technical challenge of growing high quality thin films.

The masked ion damage (MID) technique has been investigated extensively by a number of groups as a viable fabrication route to create Josephson junctions for its potential

of low production cost and high yield [9]–[11]. In our previous work, we have explored the application of Au masked 50 keV proton beam irradiation damage process for superconductor—normal—superconductor (SNS) type Josephson junctions in YBa<sub>2</sub>Cu<sub>3</sub>O<sub>7- $\delta$</sub>  (YBCO) in combination with a nanoscale focused ion beam direct milling [11]. Although these results are promising, the technique can be limited by problems associated with mask structures such as broadening effect in the definition of slot width, and nonideal geometric shape of the mask associated with high aspect ratio cut. Here, we report our latest results based on an optimized mask structure by introduction of a very thin Si buffer layer in between metal mask and the MgB<sub>2</sub> layer.

The junctions fabricated in this way display nonhysteretic, resistively shunted junction (RSJ) like current—voltage (I-V) characteristics between  $T_C$  of the tracks and 24 K. Microwave-induced steps at expected voltages and an oscillatory magnetic field dependence of critical current were observed. Junctions on the same chip show nearly identical properties over a temperature range of Josephson coupling.

## II. JUNCTION FABRICATION

Our sample preparation technique has been described elsewhere [12] and will be only briefly reviewed here. B films were first deposited at room temperature on to (0001) sapphire substrates by electron-beam evaporation and then *ex situ* annealed in a Mg vapor at 850°C for 30 min to produce 400 nm thick MgB<sub>2</sub> films. These were Ar ion beam milled to a final thickness of 120 nm and  $T_C$  of 35 K. As schematically illustrated in Fig. 1, we first defined a window area in the photoresist to which approximately 70 nm of Si layer was applied by dc magnetron sputtering at room temperature [See Fig. 1(b)]. After rinsing the photoresist, the films were coated with 360 nm thick Au on the top of Si/MgB<sub>2</sub> bilayer [Fig. 1(c)]. Tracks and contact pads were patterned in the film by conventional optical lithography [Fig. 1(d)]. The  $T_C$  of the tracks prior to further processing was measured and still found to be 35 K.

The patterned chips were then transferred to FIB system (FEI Corporation 200 xP<sup>®</sup>) for a mask aperture preparation. The Ga ion beam had a dwell time of 1  $\mu$ s, a beam spot overlap of 50%, and an acceleration beam voltage of 30 kV throughout the process. Trenches of single-pixel line were made at 4 pA in the Au. Accurate control of the milling depth was achieved by *in situ* measurements of the track resistance during milling [13] [see Fig. 1(e)]. After the metal mask aperture was prepared with FIB, the  $T_C$  of the tracks was re-measured before final implantation and was found to be unchanged.

Manuscript received August 6, 2002. This work was supported in part by the U.K. Engineering and Physical Sciences Research Council and by the Korean Ministry of Science and Technology under the National Research Laboratory Project.

D.-J. Kang is with the Department of Materials Science, University of Cambridge, Pembroke Street, Cambridge CB2 3QZ, U.K. and also with the IRC for Nanotechnology, University of Cambridge (e-mail: djk1003@cus.cam.ac.uk).

N. H. Peng, C. Jeynes, and R. Webb are with the Surrey Centre for Research in Ion Beam Applications, School of Electronics, Computing and Mathematics, University of Surrey, Guildford GU2 7XH, U.K.

H. N. Lee and B. Oh are with the LG Electronics Institute of Technology, Seoul 137-724, Korea.

S. H. Moon is with the School of Materials Science and Engineering, College of Engineering, Seoul National University, Seoul 151-744, Korea.

G. Burnell, N. A. Stelmashenko, E. J. Tarte, D. F. Moore, and M. G. Blamire are with the IRC in Superconductivity, University of Cambridge, Cambridge CB3 0HE, U.K.

Digital Object Identifier 10.1109/TASC.2003.814157

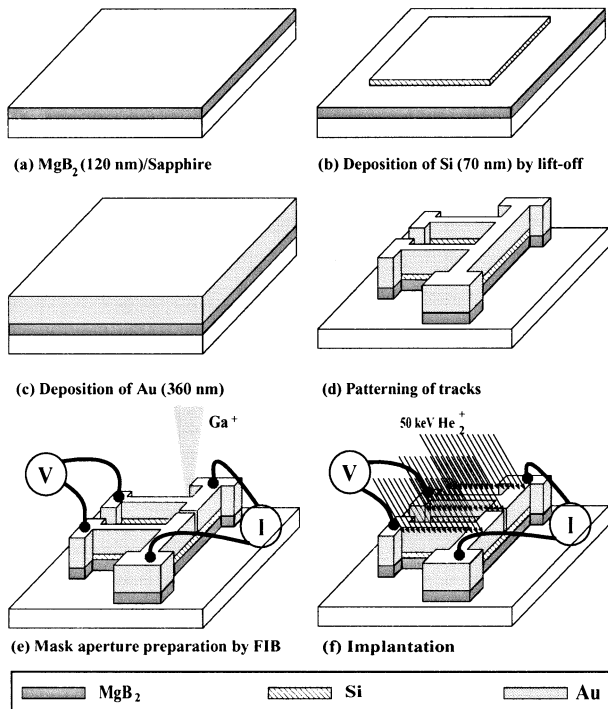


Fig. 1. Fabrication sequence for metal masked ion damage weak links.

The sample was then mounted on an ion implanter equipped with a custom-made cryogenic stage and shielded to allow ion implantation of the device through a 2 mm aperture. The *in situ* electrical measurement system and cryogenic sample stage in the implanter offer us an accurate control of the implantation process at low temperatures. We monitor the time and temperature dependence of the sample resistance during implantation. The maximum operating temperature and dosage are determined accurately by monitoring the resistance of the barrier at a given temperature and using the resistive transition as an endpoint. While monitoring the barrier resistance *in situ*, the samples are exposed to a 50 keV  $\text{H}_2^+$  ion beam with a nominal dose of up to  $4.5 \times 10^{15}$  ions/cm<sup>2</sup> at 20 K (see Fig. 1(f)). This temperature is chosen to ensure that the intended maximum operating temperature of the completed device is close to the  $T_C$  of the bulk after room temperature annealing. More detailed information on this ion beam damage technology can be found elsewhere [14].

### III. RESULTS AND DISCUSSION

After implantation, the Au on top of the Si layer was completely removed to eliminate any possible parasitic shunt resistance caused by a thick Au layer, before electrical characterizations.  $T_C$  of the tracks was re-measured at this stage and was still found to be unchanged. 6 tracks were prepared and their I-V characteristics were measured over a range of temperatures in a dip probe. Microwave radiation and magnetic field were applied to assess the quality of the junctions.

Fig. 2 shows the temperature dependence of the critical current ( $I_C$ ) of the junctions. Like focused electron beam damage junctions, the MID devices exhibit a rapid increase of  $I_C$  with

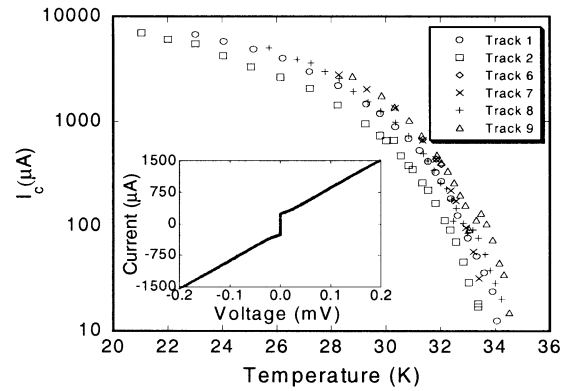


Fig. 2. Temperature dependence of critical current of a junction. Inset: current-voltage characteristics of a 3  $\mu\text{m}$  wide junction at 32 K.

temperature. This behavior is consistent with existing models of SNS junctions with soft boundary conditions [15].

Small variation of  $I_C$  with temperature from one track to another were observed even though they were on the same chip and thus, received an identical nominal implantation dose per unit area. The most likely reasons for this spread are that the degree of focus of the Ga ion beam used to prepare the metal mask apertures could vary from place to place on the substrate surface. The effect of defocus will be to broaden the milled trench; this will in turn reduce the ion dose per unit area experienced by the  $\text{MgB}_2$  film beneath and increase the effective barrier length due to the increased trench width. Film thickness variation which was often found in the same batch could also cause nonuniform critical temperature distribution and different nature of damage with the depth below the film surface in the ion-modified weak links as described by Tinchev [16]. The inset in Fig. 2 is an example of I-V characteristics of a junction at 32 K. The I-V characteristics show the RSJ model behavior with some excess current. The normal resistance was nearly temperature independent between the  $T_C$  and 24 K and was about  $0.25 \Omega$  at 32 K. At 24 K, we have  $I_C = 8$  mA and  $R_n = 0.243 \Omega$ , from which a product  $I_C R_n = 1.94$  mV is obtained. This value is still much small if compared with the value  $I_C R_n = \pi\Delta/2 = 3.52\pi k_B T_C/4 = 9.3$  mV predicted by the BCS theory for  $T_C = 39$  K. No significant change in the junction properties was observed over 2 months and a number of thermal cycles.

The Josephson nature of the  $V = 0$  branch appeared in the I-V characteristics is confirmed by the regular appearance of Shapiro steps (ac Josephson effect) when the junctions are under microwave irradiation. All tracks show clearly microwave induced constant voltage steps over a wide temperature range. The steps are observed at voltages  $V_n = n\Phi_0\nu$ , where  $n$  is an integer,  $\Phi_0$  is the flux quantum, and  $\nu$  is the frequency of the applied radiation. As expected, the voltage steps are found to be around 25  $\mu\text{V}$  for microwave power at frequency of 12 GHz. (see Fig. 3). The induced steps exhibit only a slight noise rounding. In this case, a total of 8 steps could be observed at 30.5 K, whereas up to 13 steps were seen at lower temperatures.

Fig. 4 shows the magnetic modulation of the  $I_C$  of a junction at 34 K—the apparently incomplete suppression of the  $I_C$  is largely due to the fixed voltage criterion used to assess the  $I_C$ .

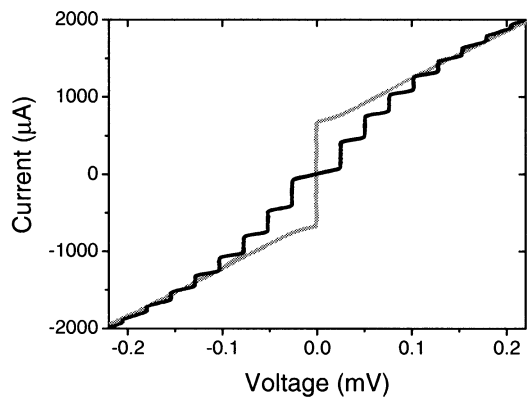


Fig. 3. Current-voltage characteristics of a 3  $\mu\text{m}$  wide junction with and without 12 GHz microwave irradiation at  $T = 30.5$  K.

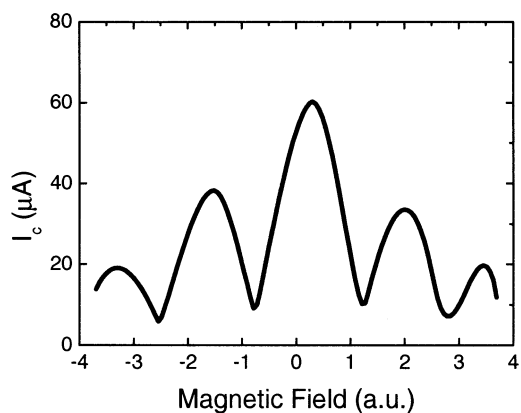


Fig. 4. Modulation of the critical current by a magnetic field applied perpendicular to the current direction, measured at 34 K.

Close to the coupling temperature of the junctions, the  $I_C$  shows a nearly complete modulation in an applied magnetic field. This indicates a homogeneous critical current density across the barrier and therefore a homogeneous defect distribution throughout the implanted region of the MgB<sub>2</sub> microbridge.

Monte Carlo simulations have been performed to investigate the effect of the Si layer thickness as a buffer layer on the formation of irradiation damage profiles inside the MgB<sub>2</sub> thin film target. Fig. 5 shows the 2 dimensional plots of simulated energy depositions (i.e., damage levels) in MgB<sub>2</sub>. The damage profile is nearly uniform in the case where 70 nm of Si layer was inserted as a buffer layer. In contrast to this, a very nonuniform damage profile is evident for buffer layer thickness of 200 nm. The simulation results clearly show that our optimized mask structure is very effective for our purposes.

As pointed out in Section I, our previous results on MID junctions fabricated with 450 nm thick Au metal mask showed some outstanding problems associated with such a thick metal mask. Firstly, the width of the irradiation damage created in mask layer is found to be wider than the nominal width of the slot created with FIB from electrical characterizations. This broadening effect was largely due to the extra mask sidewall scattering process of energetic projectiles, as revealed from our previous Monte Carlo simulation results [17]. The sidewall scattering process is intrinsic to the nanometer scale high aspect ratio masked irradi-

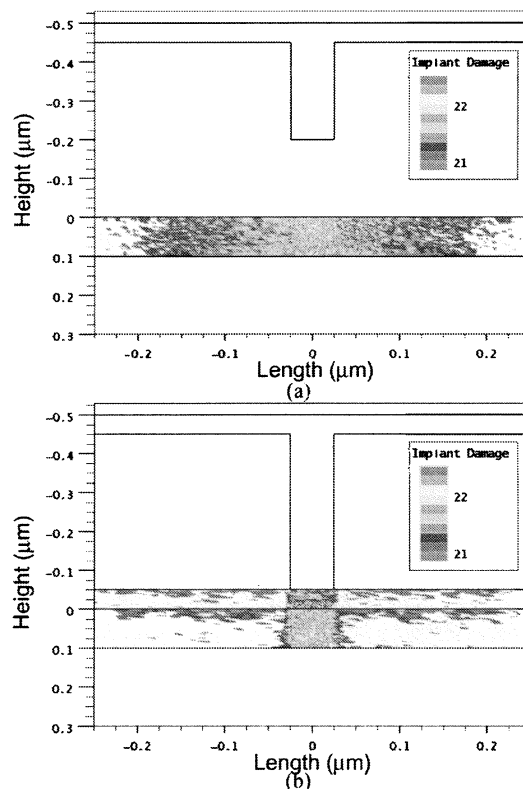


Fig. 5. Simulated 50 keV  $\text{H}_2^+$  ion beam irradiation induced energy depositions ( $\text{eV}/\text{cm}^3$ ) in model mask structures. The irradiation conditions are: 50 keV proton beam, 15 degree tilting, and dose  $2 \times 10^{16}$  ions/ $\text{cm}^2$ . (a) 450 nm amorphous Au, 200 nm Au as buffer layer, 100 nm amorphous MgB<sub>2</sub> and LaAlO<sub>3</sub> substrate (b) 380 nm amorphous Au, 70 nm poly-Si, 100 nm amorphous MgB<sub>2</sub> and LaAlO<sub>3</sub> substrate.

ation damage process, but its effect can be minimized substantially by optimizing the beam and mask properties.

A further potential problem with fabricating the mask structure with a focused Ga ion beam is with Ga diffusion into the MgB<sub>2</sub> from the masking layer during implantation: although 30 kV Ga ions have a short range in Au ( $7.6 \pm 7$  nm), irradiation can lead to increased diffusion lengths. Ga contamination may lead to a suppression of the superconducting properties, and due to the diffusive nature of the contamination will result in a broad region of suppression rather than the narrow barrier created by direct implantation damage.

To alleviate this problem we considered two approaches. We could use a thick metal mask and leave a layer of about 200 nm of Au below the bottom of the trench in which the Ga would be contained during implantation. However, this thick Ga diffusion buffer layer may destroy the high definition of the masked damage barrier layers, leading to a poor device performance.

In addition, the extra metal mask will increase the parasitic shunt conductance. An alternative approach is to insert another (preferably insulating) layer to act as a Ga diffusion barrier. An insulating layer is advantageous as it allows for endpoint detection by the *in situ* resistance measurement during mask aperture fabrication. In YBCO devices we have successfully used this approach with a SrTiO<sub>3</sub> layer, however, in MgB<sub>2</sub> oxide layers may lead to degradation of the MgB<sub>2</sub> due to the oxygen content. For MgB<sub>2</sub> we have used a 70 nm thick Si layer to act as the diffusion barrier.

Si was chosen because according to TRIM calculation, 70 nm of Si should be thick enough to prevent Ga from contaminating  $\text{MgB}_2$ , while it is thin enough, allowing ion irradiation to create desired damage profile in  $\text{MgB}_2$  target. Si is also found to be chemically compatible with  $\text{MgB}_2$ —no appreciable degradation of  $\text{MgB}_2$  over a month was observed. Finally, the Au can be readily removed after implantation since 70 nm of Si can serve as an endpoint detection layer during milling process thus eliminating problems associated with the parasitic shunt conductance due to the thick Au layer.

#### IV. CONCLUSION

In conclusion, high quality  $\text{MgB}_2$  metal masked ion beam damage Josephson junctions were successfully realized, showing RSJ-like current-voltage characteristics. Both, dc and ac Josephson effects were clearly observed by the modulation of the critical current by applied magnetic fields and the appearance of Shapiro steps under microwave irradiation. Even though we have successfully created Josephson junctions in  $\text{MgB}_2$  by irradiation damage technology, very little is known about the nature of the defects created during the implantation. Thus, the precise origin of the weak-link behavior is not well understood. In the near future, we will attempt to address this issue by studying transport properties of a series of resistors created in this way and by high-resolution transmission electron microscope investigation at the cross-section of the barrier region. With further optimization of the irradiation dose, our technique can be a very effective and convenient tool for prototyping devices due to its simplicity and flexibility of fabrication and has a great potential for high-density integration.

#### REFERENCES

- [1] J. Nagamatsu, N. Nakagawa, T. Muranaka, Y. Zenitani, and J. Akimitsu, "Superconductivity at 39 K in a magnesium diboride," *Nature*, vol. 410, pp. 63–64, Mar. 2001.
- [2] C. Buzea and N. Yamashita, "Review of the superconducting properties of  $\text{MgB}_2$ ," *Supercond. Sci. Tech.*, pp. R115–R146, Nov. 2001.
- [3] R. S. Gonnelli, A. Calzolari, D. Daghero, G. A. Ummaryno, V. A. Stepanov, G. Giunchi, S. Ceresara, and G. Ripamonti, "Josephson effect in  $\text{MgB}_2$  break junction," *Phys. Rev. Lett.*, vol. 87, 2001. art no. 097001.
- [4] Y. Zhang, D. Kinion, J. Chen, D. G. Hinks, and G. W. Crabtree, "Low-noise dc superconducting quantum interference devices," *Appl. Phys. Lett.*, vol. 79, no. 24, pp. 3995–3997, Dec. 2001.
- [5] G. Burnell, D.-J. Kang, H. N. Lee, S. H. Moon, B. Oh, and M. G. Blamire, "Planar superconductor-normal-superconductor Josephson junctions in  $\text{MgB}_2$ ," *Appl. Phys. Lett.*, vol. 70, no. 21, pp. 3464–3466, Nov. 2001.
- [6] A. Brinkman, D. Veldhuis, D. Mijatovic, G. Rijnders, D. H. A. Blank, H. Hilgenkamp, and H. Rogalla, "Superconducting quantum interference device based on  $\text{MgB}_2$  nanobridges," *Appl. Phys. Lett.*, vol. 79, pp. 2420–2422, Oct. 2001.
- [7] D. Mijatovic, A. Brinkman, I. Oomen, G. Rijnders, H. Hilgenkamp, H. Rogalla, and D. H. A. Blank, "Magnesium-diboride ramp-type Josephson junctions," *Appl. Phys. Lett.*, vol. 80, pp. 2141–2143, Mar. 2002.
- [8] Z.-Z. Li, Y. Kuan, H.-J. Tao, Z.-A. Ren, G.-C. Che, B.-R. Zhao, and Z.-X. Zhao, "Josephson tunneling in  $\text{MgB}_2$  break junctions," *Physica C*, vol. 370, no. 1, pp. 1–5, Apr. 2002.
- [9] A. S. Katz, S. I. Woods, and R. C. Dynes, "Transport properties of high  $T_c$  planar Josephson junctions fabricated by nanolithography and ion implantation," *J. Appl. Phys.*, vol. 87, no. 6, pp. 2978–2983, Mar. 2000.
- [10] F. Kahlmann, A. Engelhardt, J. Schubert, W. Zander, Ch. Buchal, and J. Hollkott, "Properties of SNS Josephson junctions fabricated by 200 keV oxygen implantation into  $\text{YBa}_2\text{Cu}_3\text{O}_{7-\delta}$ ," *IEEE Trans. Appl. Supercond.*, vol. 9, no. 2, pp. 2874–2877, June 1999.
- [11] D.-J. Kang, G. Burnell, S. J. Lloyd, R. S. Speaks, N. H. Peng, C. Jeynes, R. Webb, J. H. Yun, S. H. Moon, B. Oh, E. J. Tarte, D. F. Moore, and M. G. Blamire, "Realization and properties of  $\text{YBa}_2\text{Cu}_3\text{O}_{7-\delta}$  Josephson junctions by metal masked ion damage technique," *Appl. Phys. Lett.*, vol. 80, no. 5, pp. 814–816, Feb. 2002.
- [12] S. H. Moon, J. H. Yun, H. N. Lee, J. I. Kye, H. G. Kim, W. Chung, and B. Oh, "High critical current densities in superconducting  $\text{MgB}_2$  films," *Appl. Phys. Lett.*, vol. 79, no. 15, pp. 2429–2431, Oct. 2001.
- [13] A. Latif, W. E. Booij, J. H. Durrell, and M. G. Blamire, "Real time resistometric depth monitoring in the focused ion beam," *J. Vac. Sci. Tech. B*, vol. 18, no. 2, pp. 761–764, Mar.–Apr. 2000.
- [14] D.-J. Kang, N. H. Peng, C. Jeynes, R. Webb, J. H. Yun, S. H. Moon, B. Oh, G. Burnell, E. J. Tarte, D. F. Moore, and M. G. Blamire, "Irradiation damage technology for manufacturable Josephson junctions," *Nucl. Instrum. Meth. B*, vol. 188, pp. 183–188, Apr. 2002.
- [15] W. E. Booij, A. J. Pauza, E. J. Tarte, D. F. Moore, and M. G. Blamire, "Proximity coupling in high  $T_c$  Josephson junctions produced by focused electron beam irradiation," *Phys. Rev. B*, vol. 55, pp. 14600–14609, 1997.
- [16] S. S. Tinchev, "Critical temperature depth profiling and improvement of  $\text{YBa}_2\text{Cu}_3\text{O}_{7-\delta}$  weak link produced by ion modification," *J. Appl. Phys.*, vol. 81, pp. 324–327, Jan. 1997.
- [17] N. H. Peng, I. R. Chakarov, C. Jeynes, R. P. Webb, W. E. Booij, M. G. Blamire, and M. J. Kelly, "2D Monte Carlo simulation of proton implantation of superconducting  $\text{YBa}_2\text{Cu}_3\text{O}_{7-\delta}$  thin films through high aspect ratio Nb mask," *Nucl. Instrum. Meth. B*, vol. 164, pp. 979–985, 2000.